Supporting Information File

A Family of Fe^{3+} based Double Strand Helicates Showing Magnetocaloric Effect, Rhodamine-B Dye and DNA binding Activities

Amit Adhikary*, Himanshu Sekhar Jena and Sanjit Konar*

Department of Chemistry, IISER Bhopal, Bhopal 462066, M.P. INDIA.

Fax:+91-755-6692392; Tel: +91-755-6692336; E-mail: aadhikary87@gmail.com, skonar@iiserb.ac.in,

Synthesis of ligand H_2L: ligand H_2L was synthesized by refluxing a solution of succinic dihydrazide (1.46 g, 10 mmol) and salicylaldehyde (2.44 g, 20 mmol) in 30 mL methanol for 12 h. The solution was cooled to room temperature and the solid precipitate obtained was filtered and washed with diethyl ether, dried in vacuum to give H_2L. Yield: 85 %. Anal. calcd. (%) for $C_{18}H_{18}N_4O_4$ (bulk sample): C, 61.01; H, 5.12; N, 15.81. Found: C, 61.08; H, 4.97; N, 15.69.Selected IR data (KBr pellet; 4000 - 600 cm^{-1}): 3449(s), 3204(m), 1666(vs), 1626(m), 1566(m), 1281(s), 1049(w).

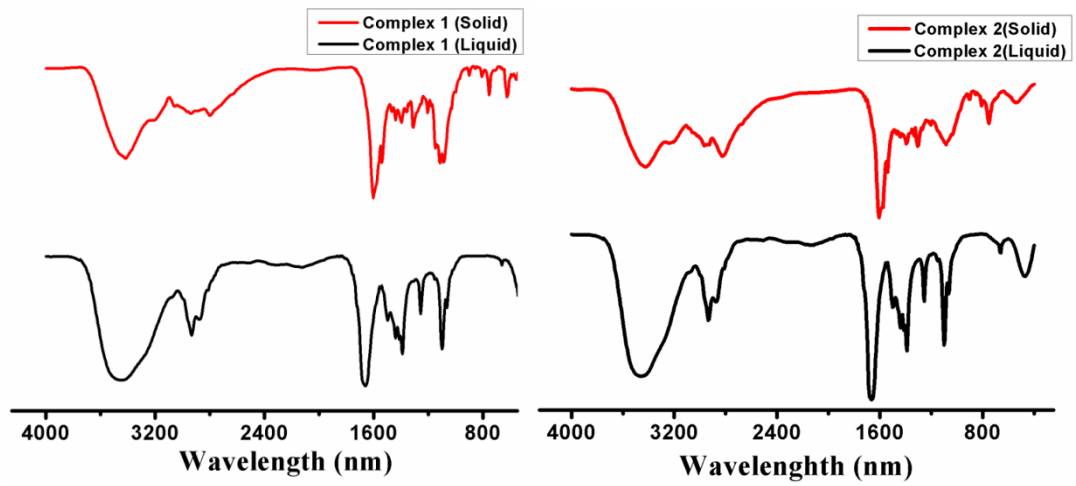

Fig. S1 FT-IR spectra of complexes **1** and **2** in solid phase and in DMF solvent.

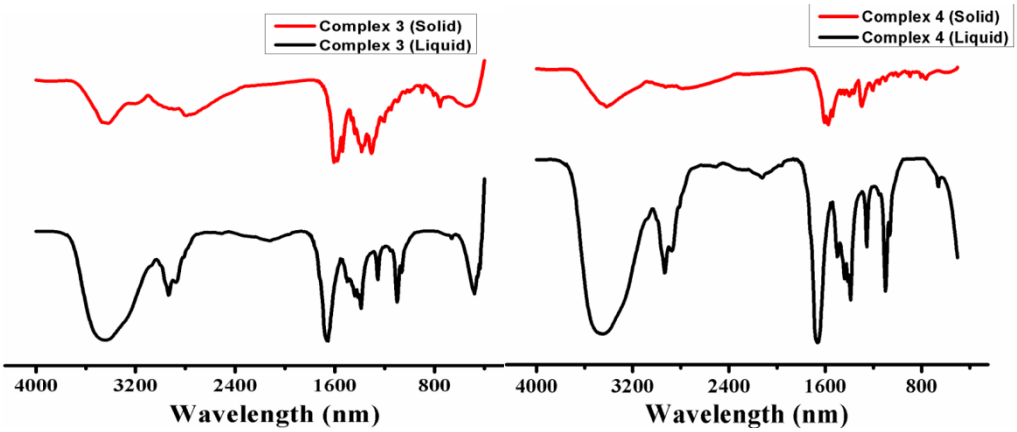

Fig. S2 FT-IR spectra of complexes **3** and **4** in solid phase and in DMF solvent.

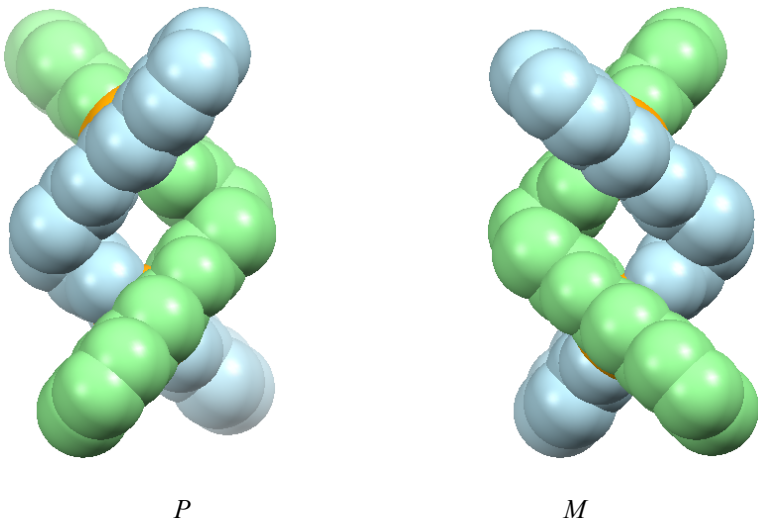

Fig. S3 Space-filling representations of the two independent cationic complexes $[Fe_2L_2]^{2+}$ found in complex **2** with *P*- and *M*- helicity.

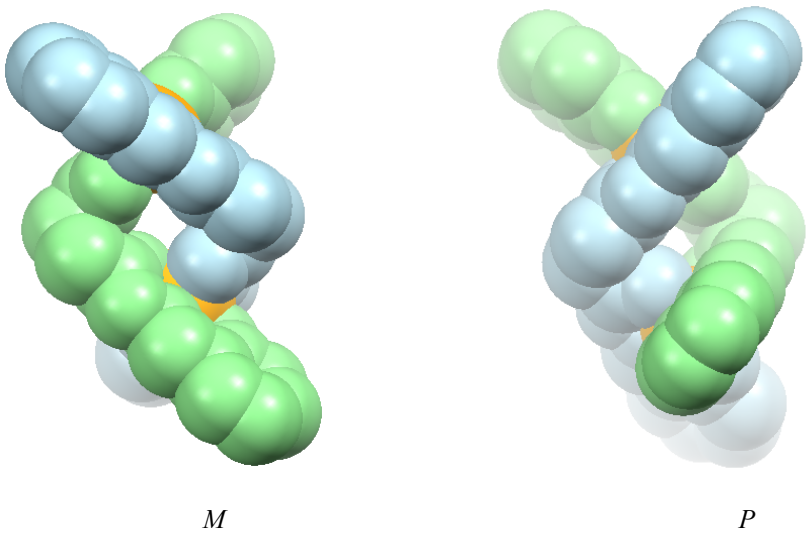

Fig. S4 Space-filling representations of the two independent cationic complexes $[Fe_2L_2]^{2+}$ found in complex **3** with *M* and *P* helicity.

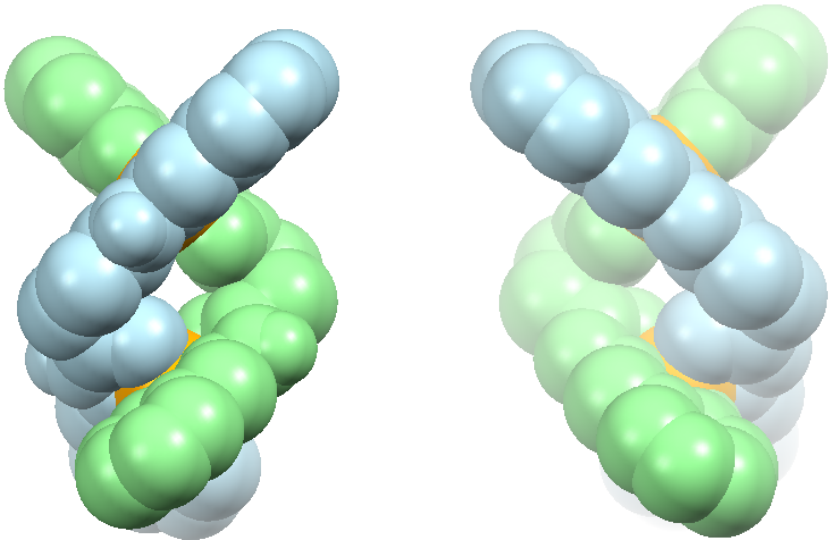

P *M*

Fig. S5 Space-filling representations of the two independent cationic complexes $[Fe_2L_2]^{2+}$ found in complex **4** with *P*- and *M*- helicity.

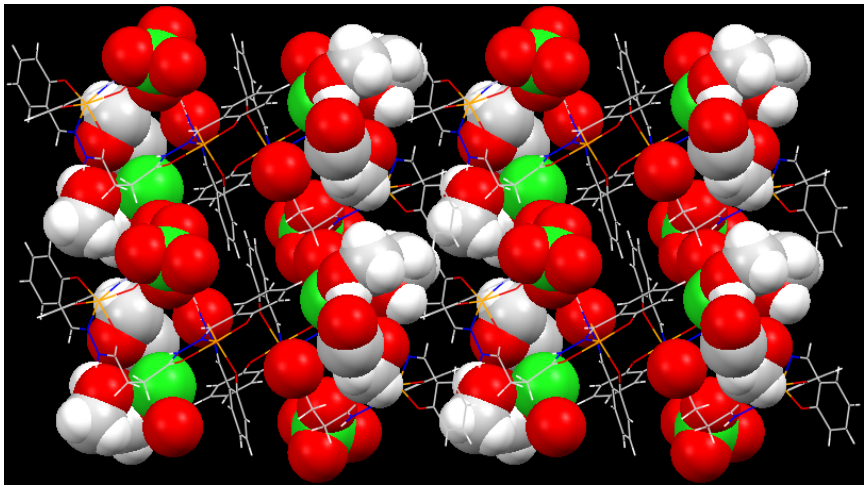

Fig. S6 A view of 1D arrangement of lattice solvents and anions through H-bonding interaction in the packing of complex **1**.

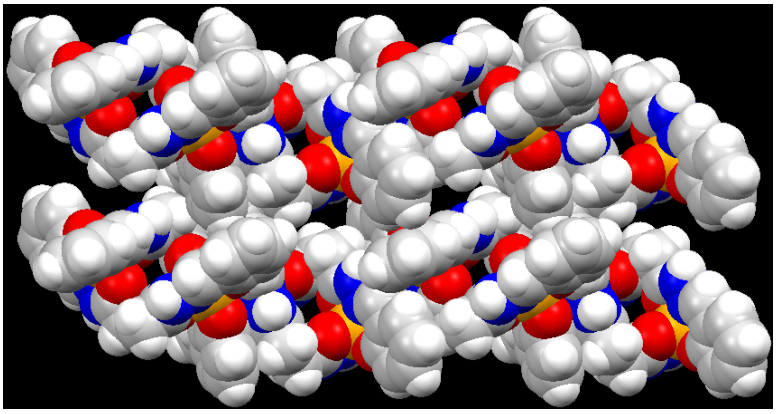

Fig. S7 A view of de-solvated de-anionic framework of **1** consisting small channels of dimensions 4.520 x 6.069 $Å^2$.

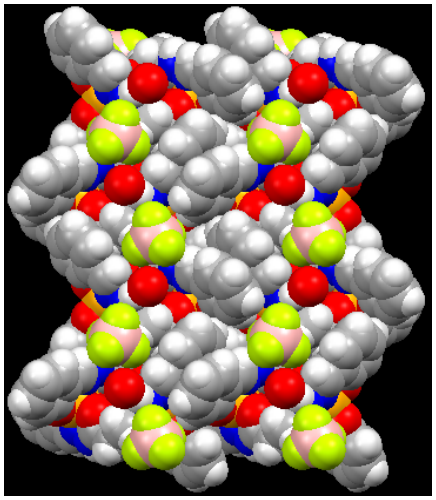

Fig. S8 Illustration of zig-zag arrangements of discrete helicates found in **2** down *a* axis.

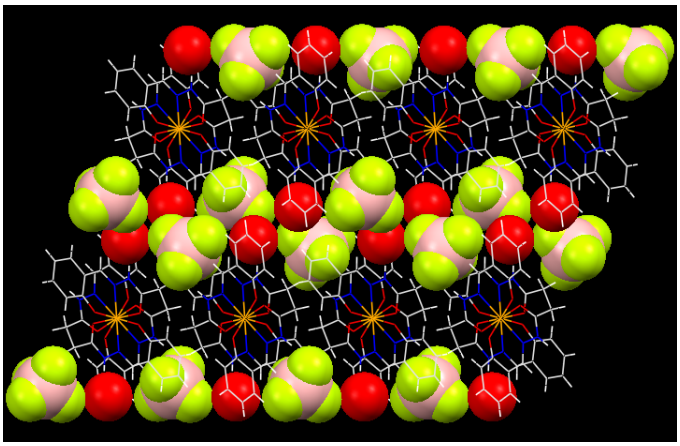

Fig. S9 A view of1D arrangement of lattice water molecules and tetrafluoroborate ions in the packing diagram of **2** down *b* axis.

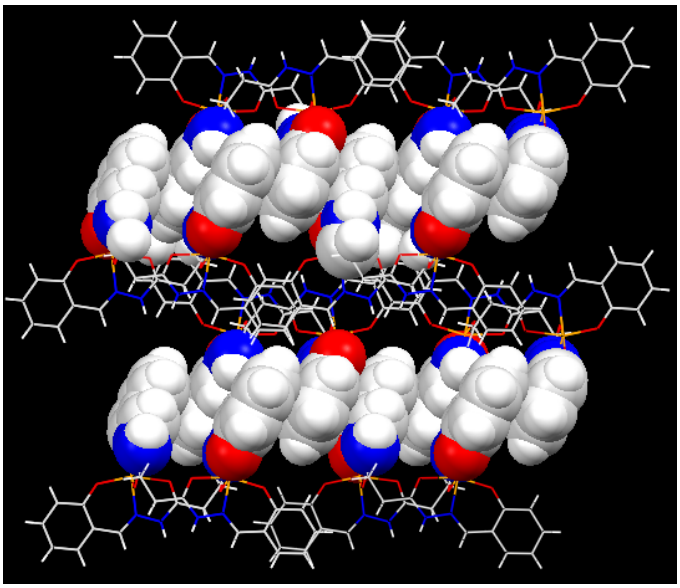

Fig. S10 A view of packing diagram of **3** emphasizing weak π···π stacking interactions (in space fill) between each discrete double helicates down *c*-axis.

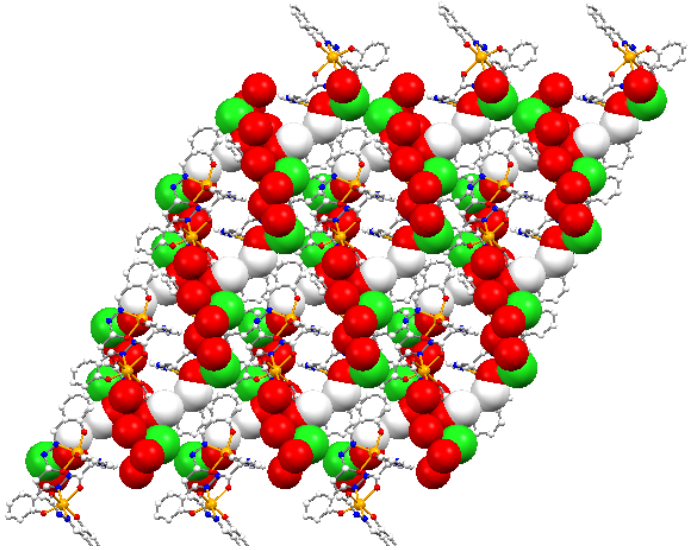

Fig. S11 A view of packing diagram of **4** illustrating the continuous rectangular arrangement of lattice solvent and chloride ions down *c*-axis.

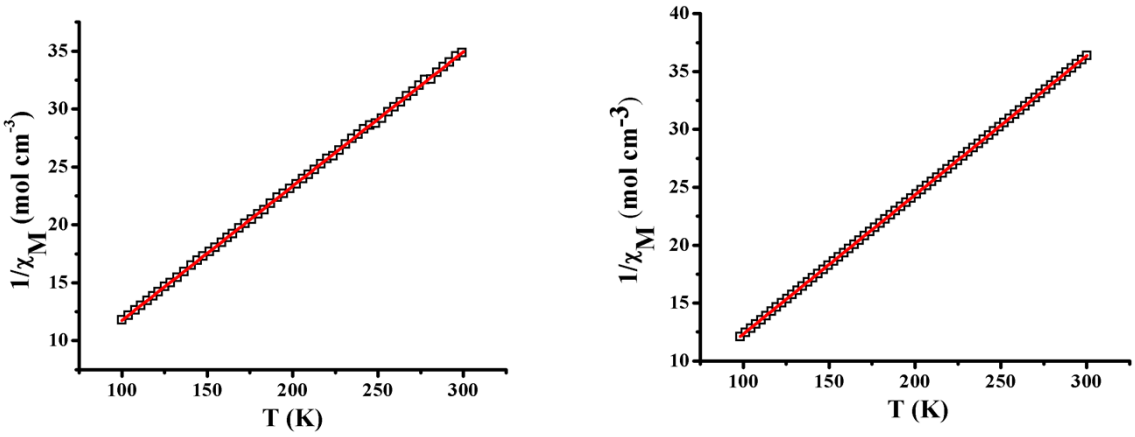

Fig. S12 $1/\chi_M$ vs T plot of complex **1** (left) and complex **2** (right) in the temperature range of 100 -300 K. Red lines indicate Curie-Weiss fitting of the plot.

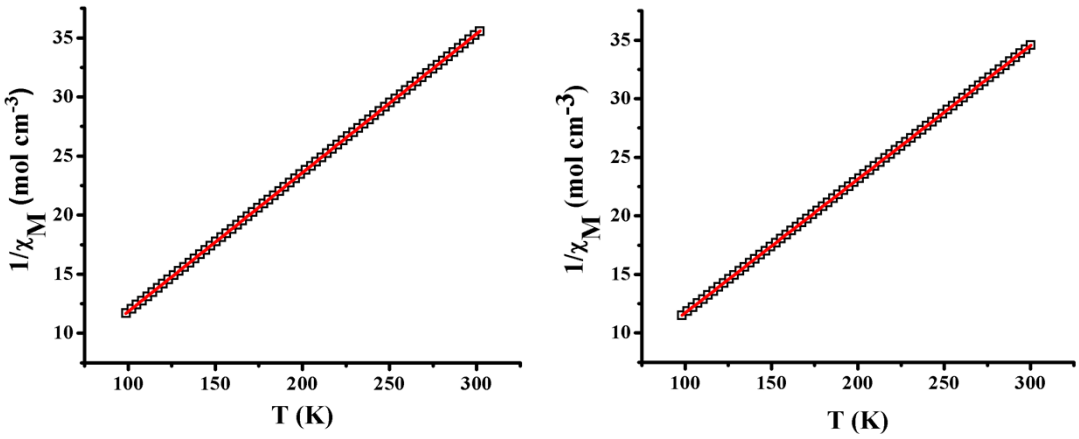

Fig. S13 $1/\chi_M$ vs T plot of complex **3** (left) and complex **4** (right) in the temperature range of 100 -300 K. Red lines indicate Curie-Weiss fitting of the plot.

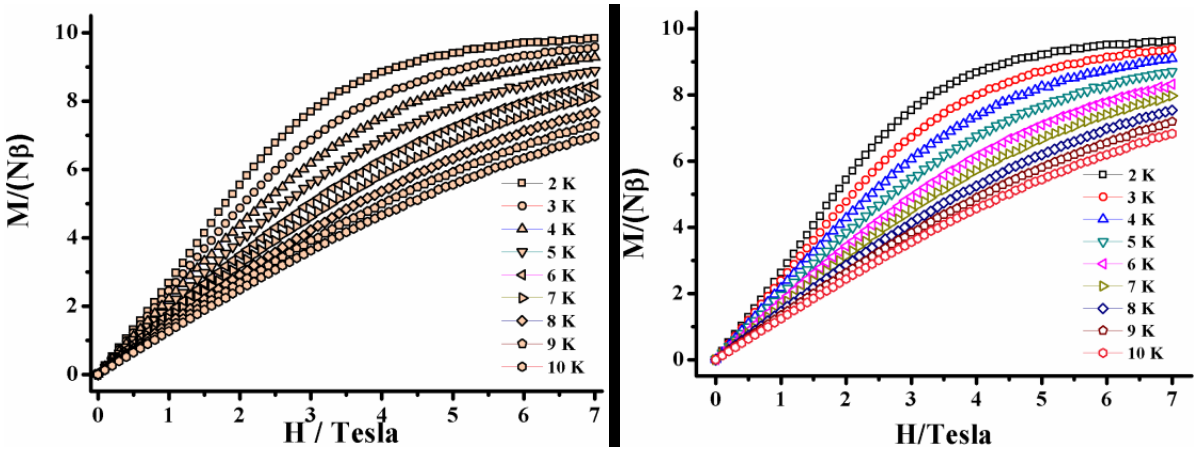

Fig.S14 Field-dependencies of isothermal normalized magnetizations for complex **2** (left) and **3** (right) collected for temperatures ranging from 2 to 10 K.

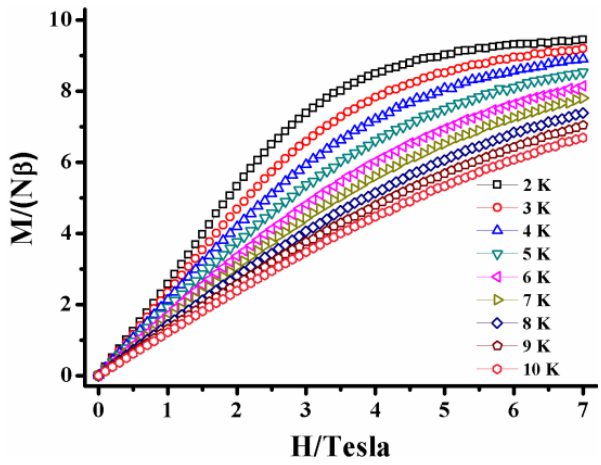

Fig.S15 Field-dependencies of isothermal normalized magnetizations for complex **4** collected for temperatures ranging from 2 to 10 K.

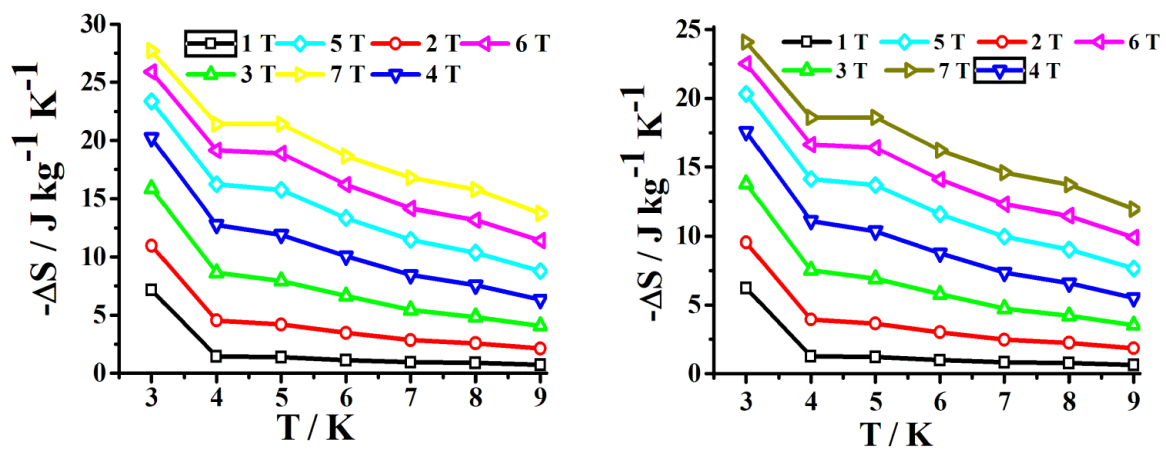

Fig. S16 Temperature dependencies (3 K to 10 K) of magnetic entropy change ($-\Delta S_m$) of complexes **2** (left) and **3** (right) as obtained from magnetization data.

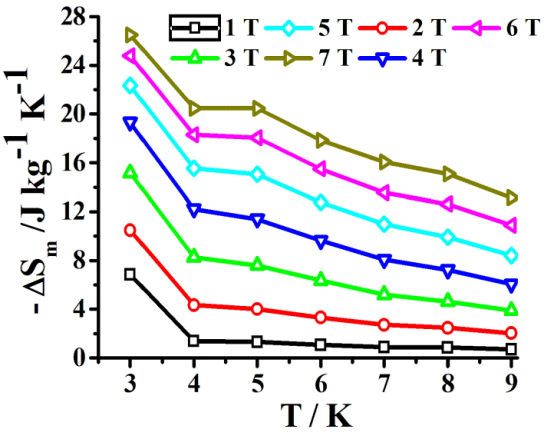

Fig. S17 Temperature dependencies (3 K to 10 K) of magnetic entropy change ($-\Delta S_m$) of complex **4** as obtained from magnetization data.

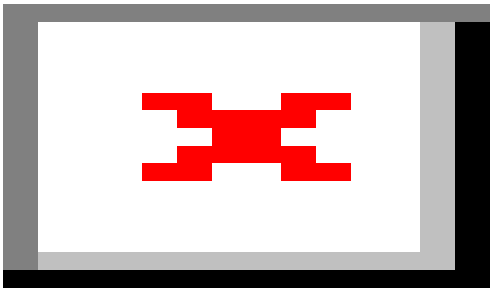

Fig. S18 Isotropic distribution pattern of observed (top) and predicted (bottom) ESI-MS of $[Fe_2L_2]^{2+}$ unit of complex **1**.

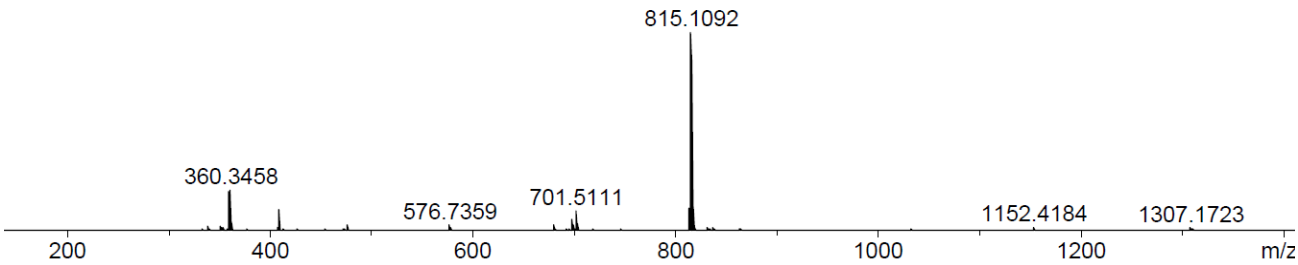

Fig. S19 ESI-MS analysis of complex **1**.

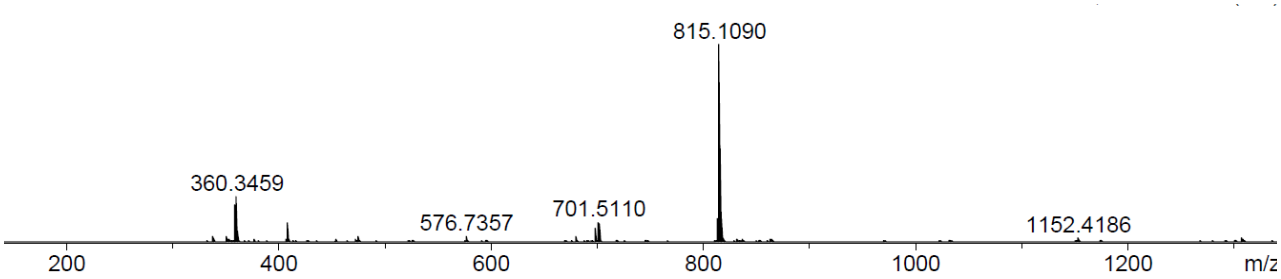

Fig. S20 ESI-MS analysis of complex **2**.

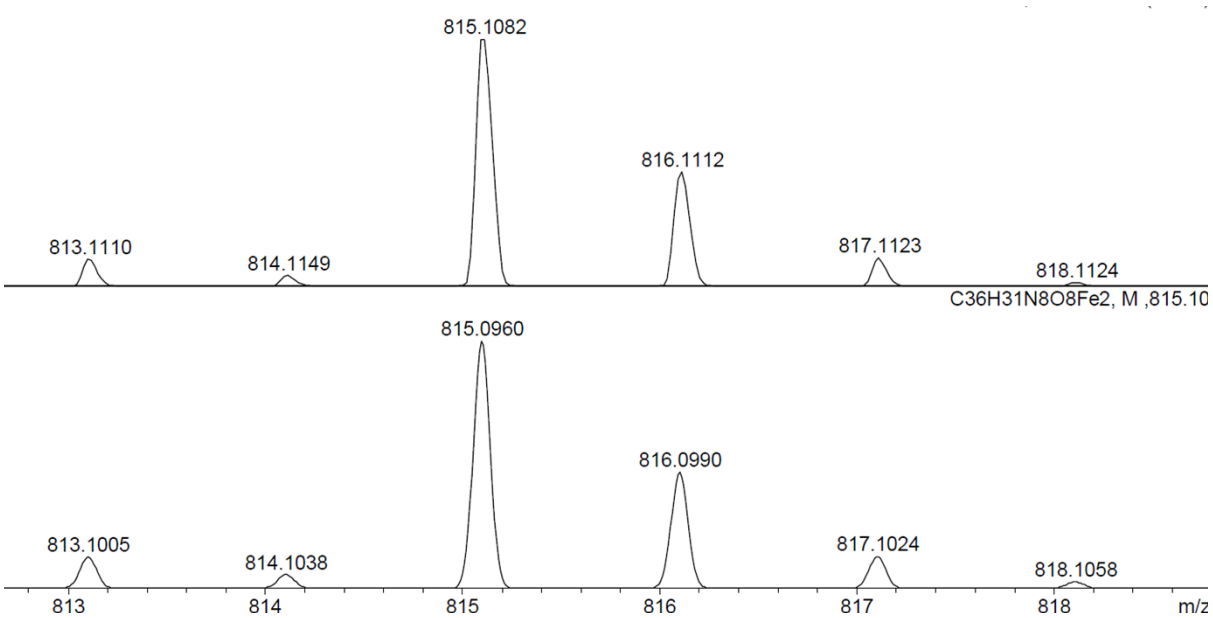

Fig. S21 Isotropic distribution pattern of observed (top) and predicted (bottom) ESI-MS of dication $[Fe_2L_2]^{2+}$ of complex **2**.

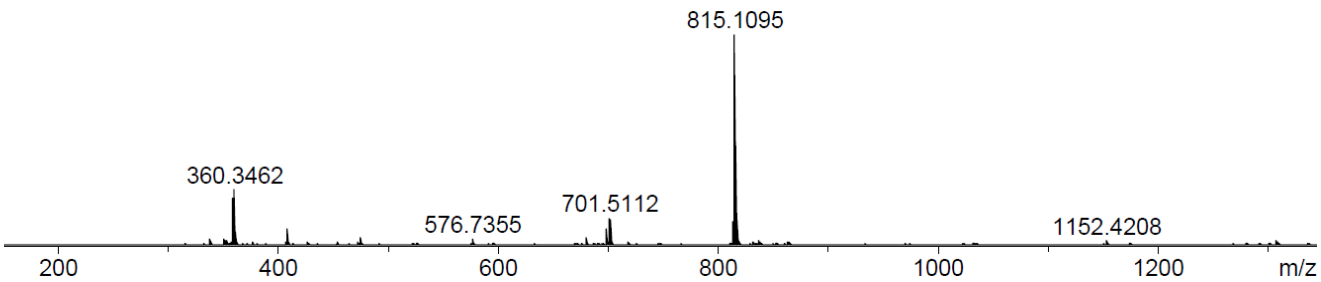

Fig. S22 ESI-MS analysis of complex **3.**

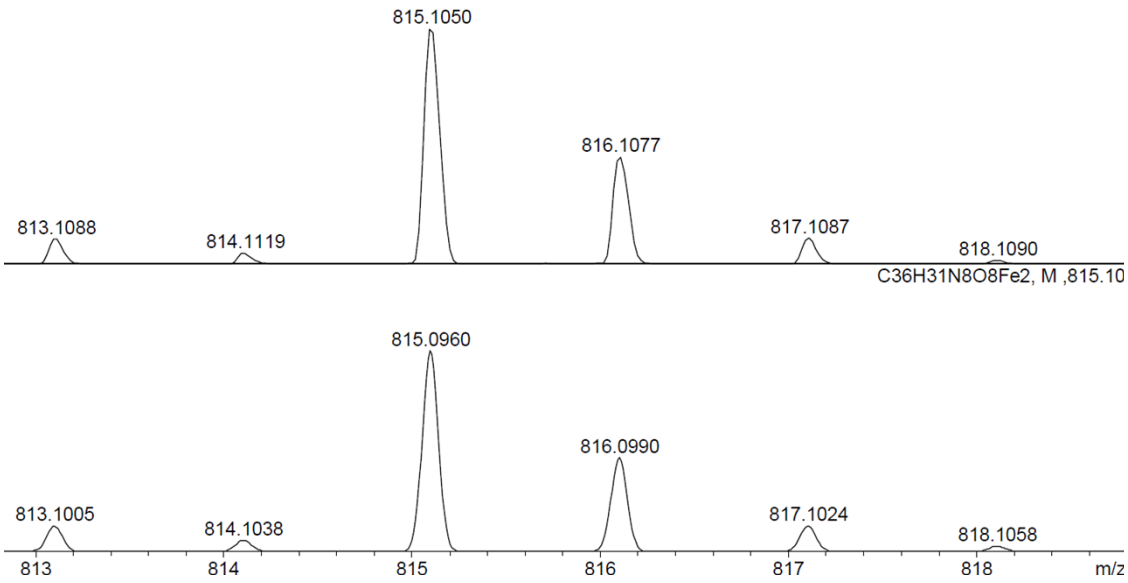

Fig. S23 Isotropic distribution pattern of observed (top) and predicted (bottom) ESI-MS of dication $[Fe_2L_2]^{2+}$ of complex **3**.

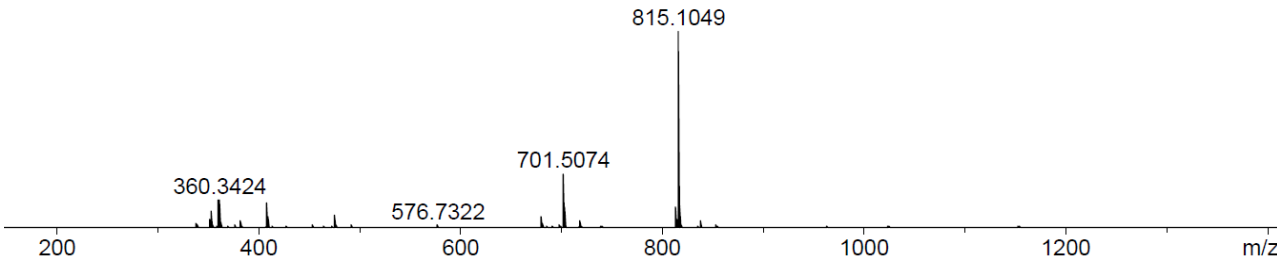

Fig. S24 ESI-MS analysis of complex **4**.

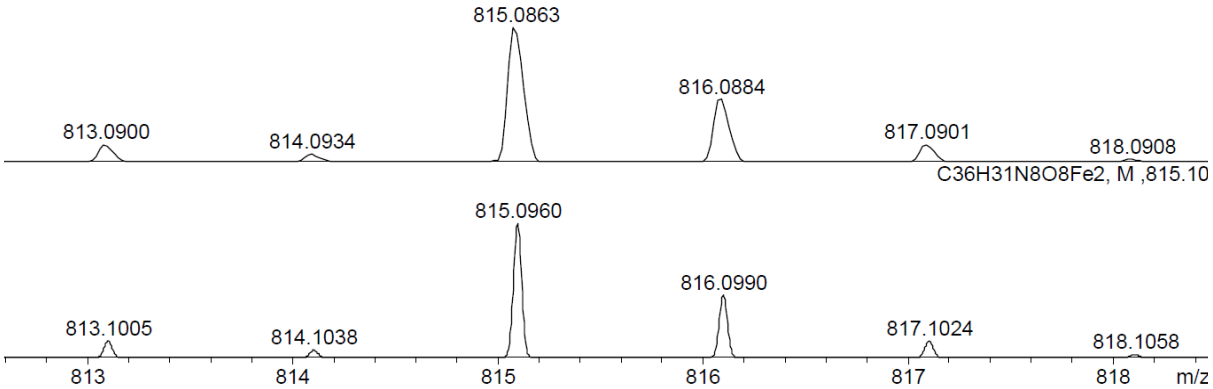

Fig. S25 Isotropic distribution pattern of observed (top) and predicted (bottom) ESI-MS of dication $[Fe_2L_2]^{2+}$ of complex **4**.

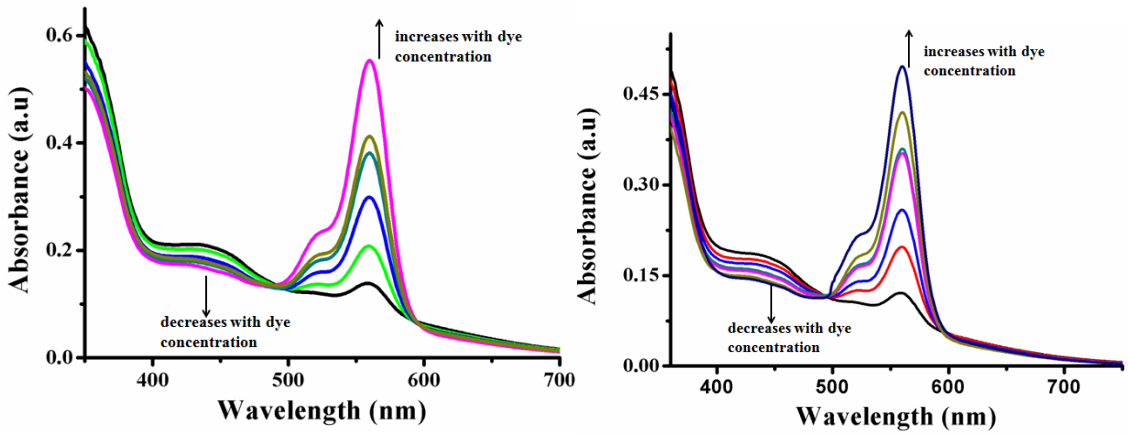

Fig. S26 UV spectra of Rhodamine-B encapsulated complex **2** (left) and **3** (right) in DMF.

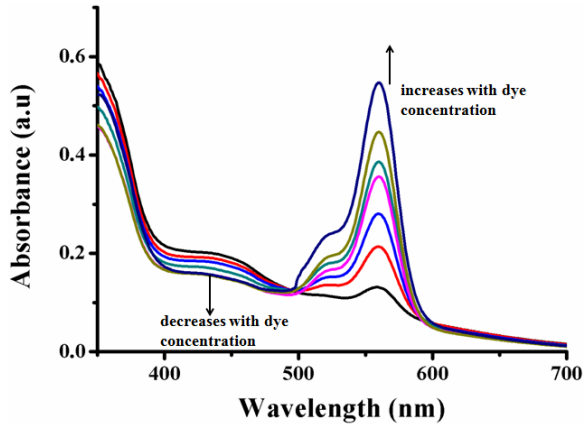

Fig. S27 UV spectra of Rhodamine-B encapsulated complex **4** in DMF.

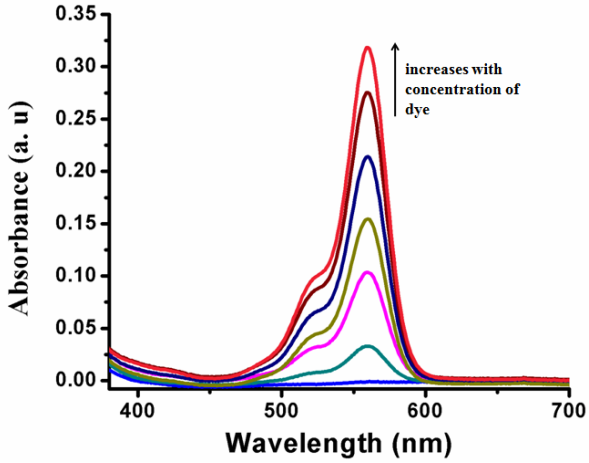

Fig. S28 UV spectra of Rhodamine-B encapsulated ligand H_2L in DMF.

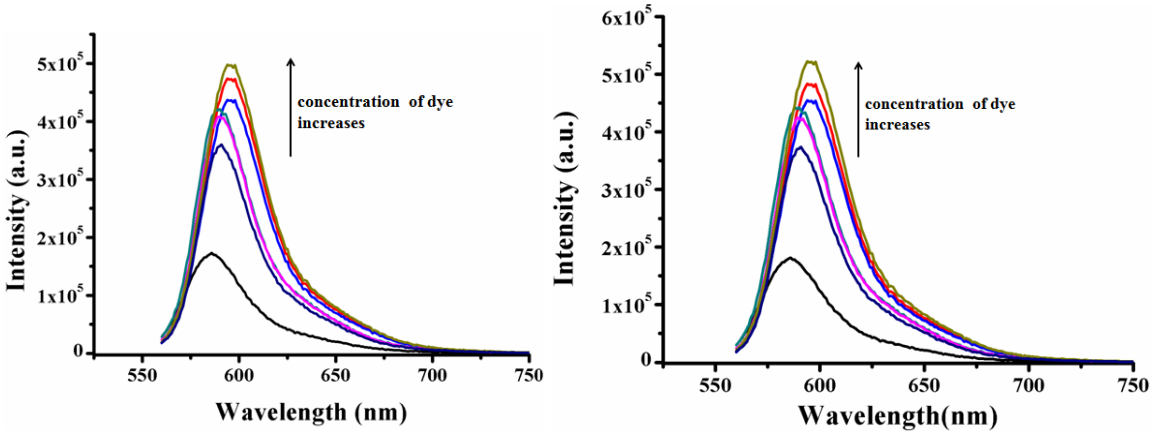

Fig. S29 Fluorescence spectra of Rhodamine-B encapsulated complex **2** (left) and **3** (right) in DMF.

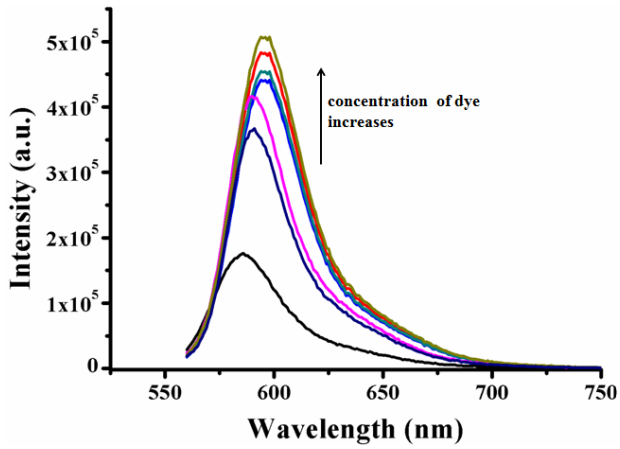

Fig. S30 Fluorescence spectra of Rhodamine-B encapsulated complex **4** in DMF.

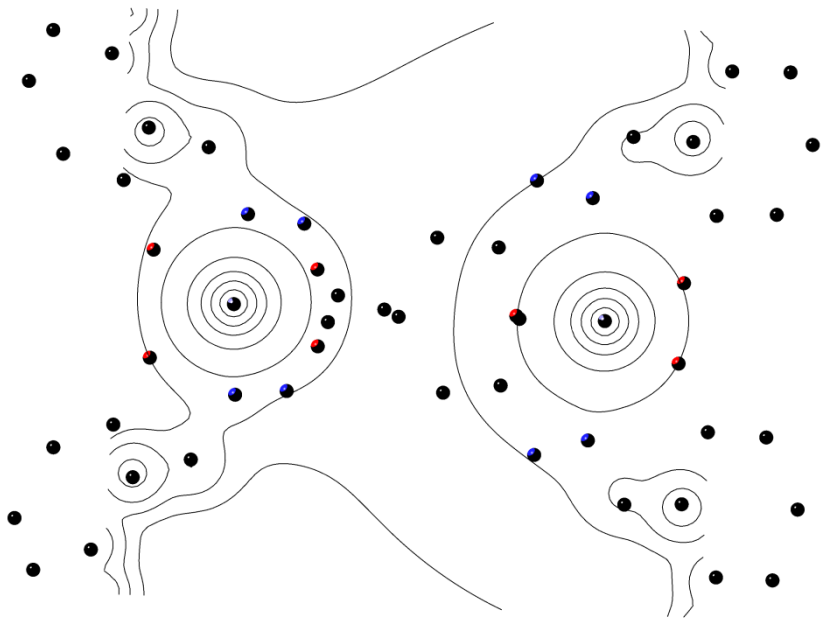

Fig. S31 Contour diagram of di-cationic structure of complexes **1-4**.

Table S1. Bond Valence Sum (BVS) calculations for complexes 1-2.

Complex 1			Complex 2		
Fe site	**BVS**	**Assigned Oxidation State**	**Fe site**	**BVS**	**Assigned Oxidation State**
Fe1	2.97	3	Fe1	2.91	3
Fe2	2.95	3	Fe2	2.88	3
Fe site	**BVS**	**Assigned Oxidation State**	**Fe site**	**BVS**	**Assigned Oxidation State**
Fe1	2.99	3	Fe1	2.86	3
Fe2	2.94	3	Fe2	2.94	3

Table S2. Selected bond distances (Å) and bond angles (deg) found in complex 1.

Complex 1			
Fe1 - N1	2.118(4)	Fe2 - O3	2.090(3)
Fe2 - N4	2.091(4)	Fe2 - O4	1.902(2)
Fe1 - N5	2.125(4)	Fe1 - O5	1.898(3)
Fe2 - N8	2.099(4)	Fe1 - O6	2.086(3)
Fe1 - O1	1.898(3)	Fe2 - O7	2.099(3)
Fe1 - O2	2.080(3)	Fe2 - O8	1.902(3)
O1 - Fe1·-·N1	84.9(1)	O6·-·Fe1·-·N5	74.7(1)
O1·-·Fe1·-·N5	115.4(1)	N1·-·Fe1·-·N5	156.6(1)
O1·-·Fe1·-·O2	159.9(1)	O3·-·Fe2·-·N4	75.2(1)
O1·-·Fe1·-·O5	91.6(1)	O3·-·Fe2·-·N8	86.9(1)
O1·-·Fe1·-·O6	92.0(1)	O3·-·Fe2·-·O4	159.8(1)
O2·-·Fe1·-·N1	75.2(1)	O3·-·Fe2·-·O7	89.1(1)
O2·-·Fe1·-·N5	84.6(1)	O3·-·Fe2·-·O8	92.2(1)
O2·-·Fe1·-·O5	91.9(1)	O4·-·Fe2·-·N8	112.6(1)
O2·-·Fe1·-·O6	92.0(1)	O4·-·Fe2·-·N4	84.6(1)
O3·-·Fe1·-·N4	75.2(1)	O4·-·Fe2·-·O7	90.7(1)
O3·-·Fe1·-·N8	86.9(1)	O4·-·Fe2·-·O8	95.1(1)
O3·-·Fe1·-·O4	159.8(1)	O7·-·Fe2·-·N4	95.2(1)
O3·-·Fe1·-·O7	89.1(1)	O7·-·Fe2·-·N8	74.8(1)
O3·-·Fe1·-·O8	92.2(1)	O7·-·Fe2·-·O8	159.1(1)
O5·-·Fe1·-·N1	107.9(1)	O8·-·Fe2·-·N4	105.3(1)
O5·-·Fe1·-·N5	84.3(1)	O8·-·Fe2·-·N8	84.4(1)
O5·-·Fe1·-·O6	158.1(1)	N4·-·Fe2·-·N8	159.8(1)
O6·-·Fe1·-·N1	94.0(1)		

Table S3. Selected bond distances (Å) and bond angles (deg) found in Complex 2.

Complex 2			
Fe3 – O3	2.102	Fe4 – O1	1.895
Fe3 – O4	1.836	Fe4 – O2	2.077
Fe3 – N4	2.101	Fe4 – N1	2.125

O1 – Fe4 - N1	85.3	O3 – Fe3 - N4	75.0
O1 – Fe4 - O2	159.9	O3 – Fe3 -O4	161.0
N1 – Fe4 - O2	74.7	N4 – Fe3 - O4	86.1

Table S4. Selected bond distances (Å) and bond angles (deg) found in complex 3.

Complex 3			
Fe1 – O3	1.891(5)	Fe2 – O5	1.899(5)
Fe1 – O4	2.084(6)	Fe2 – O6	2.077(5)
Fe1 – O7	2.069(5)	Fe2 – O2	1.901(6)
Fe1 – O8	1.913(4)	Fe2 – O1	2.105(5)
Fe1 - N1	2.127(6)	Fe2 – N6	2.118(5)
Fe1 - N5	2.094(5)	Fe2 - N8	2.094(5)
O7 - Fe1 – O8	158.8(2)	O1 – Fe2 – O2	157.1(2)
N1 - Fe1 – O4	74.4(2)	O6 – Fe2 – O1	85.3(2)
O7 - Fe1 – O4	92.9(2)	O5 – Fe2 – O1	96.5(2)
O3 - Fe1 – O4	157.5(2)	O5– Fe2 – O2	96.3(2)
O3 - Fe1 – 08	92.3(2)	O6 – Fe2 – N8	105.4(2)
O7 - Fe1 – N1	86.5(2)	O5 – Fe2 – N8	94.7(2)
O4 - Fe1 – O8	90.2(2)	O6 – Fe2 – O5	159.5(2)
O4 - Fe1 – N4	87.0(2)	O2 – Fe2 – N8	85.3(2)
O8 - Fe1 – N1	114.5(2)	O1 – Fe2 – N6	87.2(2)
O8 - Fe1 – N4	84.5(2)	O5 – Fe2 – N6	84.6(2)
O7 - Fe1 – N4	74.7(2)	O6 – Fe2 – N6	75.1(2)
N1 - Fe1 – N4	152.9(2)	N6 – Fe2 – N8	161.8(2)

Table S5. Selected bond distances (Å) and bond angles (deg)found in complex 4.

Complex 4			
Fe1 - O1	1.909(2)	Fe2 - O3	2.125(3)
Fe1 - O2	2.103(2)	Fe2 - O4	1.891(3)
Fe1 - O5	1.892(3)	Fe2 - O7	2.106(2)
Fe1 - O6	2.105(3)	Fe2 - O8	1.899(2)
Fe1 - N1	2.117(2)	Fe2 - N4	2.105(3)
Fe1 - N5	2.123(2)	Fe2 - N8	2.116(3)
O1 - Fe1 - O2	155.2(9)	O3 - Fe2 - O4	158.6(1)
O1 - Fe1 - O5	101.3(1)	O3 - Fe2 - O7	85.3(9)
O1 - Fe1 - O6	86.2(1)	O3 - Fe2 - O8	90.2(1)
O1 - Fe1 – N1	84.5(1)	O3 - Fe2 - N4	74.9(9)
O1 - Fe1 – N5	112.9(1)	O3 - Fe2 - N8	98.7(1)
O2 - Fe1 – O5	93.9(1)	O4 - Fe2 - O7	92.0(1)
O2 - Fe1 - O6	86.8(9)	O4 - Fe2 - O8	99.(1)
O2 - Fe1 – N1	74.9(9)	O4 - Fe2 - N4	84.6(1)
O2 - Fe1 – N5	87.9(1)	O4 - Fe2 - N8	101.0(1)
O5 - Fe1 - O6	158.3(1)	O7 - Fe2 - O8	158.5(1)
O5 - Fe1 – N1	94.2(1)	O7 - Fe2 - N4	99.2(9)
O5 - Fe1 - N5	84.2(1)	O7 - Fe2 - N8	74.7(9)

O6 - Fe1 – N1	106.9(9)	O8 - Fe2 - N4	99.9(1)
O6 - Fe1 – N5	74.1(9)	O8 - Fe2 - N8	85.2(1)
N5 - Fe1 – N1	162.5(1)	N4 – Fe2 – N8	171.8(1)

Table S6. Selected hydrogen bonding distances (Å) and angles (deg) for the complexes 1-4.

D-H….A	Symmetry operation	D-H(Å)	H…A(Å)	D….A(Å)	<D-H-A>(deg)
		Complex 1			
N6-H6….O3	x,y,z	0.860	1.874	2.722	168.72
N3-H3….O15	x,y,z	0.860	1.697	2.670	157.83
N2-H2...O17	-x+1,-y+1,-z	0.860	1.825	2.673	168.66
N7-H7...O18	x-1,+y,+z	0.860	1.900	2.672	148.52
O14-H14A...O15	x+1,+y,+z	0.820	2.698	3.112	113.01
O17-H17A...O16	x+1,+y,+z	0.820	1.936	2.682	150.81
O15-H15A...Cl2	-x+1,-y+1,-z	0.820	2.259	3.060	165.53
O18-H18A...Cl2	-x+1,-y+1,-z	0.850	2.594	3.156	124.66
O16-H16A...Cl2	-x+1,-y+1,-z+1	0.820	2.482	3.051	127.46
O18-H18B...O9	x+1,+y,+z	0.850	2.033	2.882	177.79
O13-H13A...O10	x,+y+1,+z	0.850	2.798	3.595	156.91
O13-H13A...O12	x,+y+1,+z	0.850	2.185	2.811	130.31
		Complex 2			
C12-H5A…F4	x,-y+1,+z+1/2	0.930	2.785	3.508	135.30
O5-H10B…F1	x,y,z	0.850	2.395	2.756	104.17
C7-H7...F3	-x,-y+1,-z	0.930	2.777	3.160	105.83
C12-H12…F2	x,-y+1,+z+1/2	0.930	2.536	3.379	180.83
C5-H5…F2	x,-y+1,+z+1/2	0.930	2.667	3.543	157.29
N2-H2…O5	x,-y+1,+z+1/2	0.860	1.926	2.766	164.80
C9-H9A…F4	-x,+y,-z+1/2	0.970	2.857	3.620	136.22
C9-H9A…F3	-x,+y,-z+1/2	0.970	2.406	3.347	163.44
C17-H17…F4	x,+y+1,+z	0.930	2.897	3.551	139.36
		Complex 3			
N6-H6…O11	x,y,z	0.880	1.853	2.717	167.0
N3-H3A…O16	-x+1,-y,-z+2	0.880	1.79	2.67	175.1
N7-H7A…O15	x,+y+1,+z	0.880	1.793	2.669	175.0
N2-H2...O18	-x+1,-y+1,-z+1	0.880	1.856	2.713	164.1
O18-H18...O13	-x+1,-y+1,-z+1	0.830	1.81	2.62	162.0
C52-H52...O16	-x+1,-y+1,-z+1	0.950	2.313	3.055	134.46
C48-H48..O10	x,y,z	0.950	2.697	3.211	114.56
C40-H40B..O17	x,+y,+z-1	0.950	2.599	3.081	111.82
		Complex 4			

O15-H15A…Cl1	x,y,z	0.870	2.254	3.118	172.37
O10-HC…Cl2	x,y,z	0.840	2..181	3.019	176.41
O11-HD…O9	x,y,z	0.870	1.998	2.878	156.16
O12-HG…Cl1	1	0.870	2.319	3.182	171.98
O13-HH…Cl2	x,y,z	0.870	2.301	3.238	177.28
N2-HJ…O12	x,y,x	0.880	1.823	2.699	173.29
N3-HK…O10	x,y,z	0.880	1.844	2.722	176.18
C7-HR…O1AA1	x,y,z	0950	2.742	3.061	100.50
O15-HA…O13	2	0.870	1.903	2.763	169.58
O13-HI…O1	6	0.870	2.142	2.991	165.06
O13-HI…O6	6	0.870	2.502	3.052	121.83
O11-HE…O15	4	0.950	1.922	2.656	141.05
O12-HF…Cl2	5	0.870	2.233	3.156	167.99
N6-HL…Cl1	7	0.880	2.301	3.164	166.69
N7-HM…O11	8	0.950	1.813	2.691	174.89
C14-HX…O7	10	0.950	2.523	3.196	127.89
C32-H18A…O4	13	0.950	2.573	3.157	119.98
O9-HB…Cl1	1	0.840	2.633	3.263	132.91

Table S7. Mulliken atomic spin densities of dication $[Fe_2L_2]^{2+}$ for HS =11 in B3LYP geometry.

	Atom	Spin densities
1	Fe	4.03823
2	O	0.24736
3	O	0.09495
4	N	0.07559
5	N	0.13206
6	O	0.22781
7	O	0.31584
8	C	0.06322
9	C	0.0215
10	N	0.15603
11	C	-0.07625
12	C	-0.08956
13	N	0.21755
14	C	0.01011
15	C	0.06805
16	C	0.21155
17	C	0.11948
18	C	-0.00399
19	H	-0.00345
20	H	0.00215
21	C	0.20395
22	C	0.00379
23	C	0.05444
24	C	-0.12218
25	C	-0.06489
26	H	-0.00814
27	H	0.00166

28	H	0.00407
29	C	0.00972
30	C	-0.10829
31	C	0.00328
32	H	0.00219
33	H	0.0032
34	H	-0.00415
35	C	-0.00267
36	H	0.00596
37	C	0.27565
38	H	0.00275
39	C	-0.04009
40	H	-0.00211
41	H	-0.00549
42	H	0.00563
43	C	0.18367
44	H	0.00241
45	H	0.00492
46	C	0.02115
47	H	1.36E-4
48	H	-0.0169
49	O	-0.01377
50	N	-0.28377
51	H	-0.01136
52	N	0.28854
53	O	0.23393
54	Fe	4.79998
55	N	-0.04858
56	N	0.24285
57	O	0.10787
58	O	0.32081
59	C	0.05923
60	C	-0.05997
61	C	-0.11508
62	C	0.07694
63	C	-0.1327
64	H	0.00475
65	C	0.189
66	H	0.00948
67	C	0.04045
68	C	0.03936
69	C	0.06975
70	C	-0.08901
71	H	-0.00133
72	C	-0.05443
73	C	0.02137
74	H	-0.00324
75	H	-0.00284
76	C	-0.09381
77	C	0.15997
78	H	0.00457
79	H	0.00438
80	H	-0.00115
81	H	0.00589

Table S8. Summarization of results obtained from DFT calculation.

Method	B3LYP
Spin	HS (M_s = 5)
$<S^2>$	31.0640
Energy(UB3LYP)	-2674.57171392
Convergence	0.1489D -7